ORGANOMETALLICS

Article

Cite This: *Organometallics* XXXX, XXX, XXX–XXX

Metal-Free Carbonylation Route to a Reactive Borataepoxide System

Tongdao Wang, Gerald Kehr, Constantin G. Daniliuc, and Gerhard Erker*

Organisch-Chemisches Institut, Westfälische Wilhelms-Universität Münster, Corrensstraße 40, 48149 Münster, Germany

Supporting Information

ABSTRACT: Hydroboration of *N*-allyl-*cis*-2,6-dimethylpiperidine with $HB(C_6F_5)_2$ gave the trimethylene-bridged frustrated N/B Lewis pair **7**. It featured a *trans*-2,6-dimethyl substitution pattern at the piperidine unit which indicated preceding equilibration with its iminium cation/hydridoborate isomer **6** by means of an internal hydride transfer. In situ generated compound **6** is essential for the reaction with $CO/HB(C_6F_5)_2$ to give the borataepoxide product **12** at the $[N]-(CH_2)_3-[B]$ framework. The borataepoxide **12** reacts rapidly with CO_2, cleaves the acidic C–H bond of a terminal alkyne, splits dihydrogen, and reacts with nitriles and benzaldehyde. Most products were characterized by X-ray diffraction.

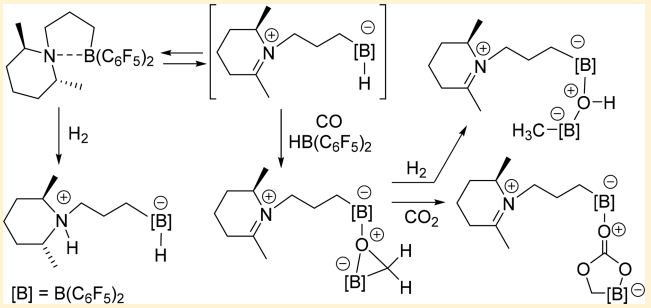

INTRODUCTION

Frustrated Lewis pairs (FLPs) are composed of Lewis acid and base components that use sterically bulky substituents in order to hinder their neutralizing Lewis adduct formation.[1] The resulting pairs of the active Lewis acid and base components have attracted some current interest as they provide effective means of small molecule activation in the absence of metal containing components.[2] In a way, FLPs often undergo reactions reminiscent of metal complex chemistry, but in a metal-free arrangement.[3] The majority of the FLP systems described so far contain P/B or N/B Lewis base/acid combinations.[2,4−6] Other combinations are less often encountered.[7,8] This also holds for oxygen/boron FLPs. There have been a few systems where the involvement of in situ generated O/B pairs[9] plays a role, but true isolated active O/B FLPs are still rare.

We had recently disclosed a novel approach to frustrated oxygen/borane Lewis pairs.[10] For this purpose, we used the reactive zirconium hydride reagent **1** (which we had readily prepared from $Cp^*_2ZrH_2$[11] and the sufficiently Brønsted acidic 2,4,6-trimethylphenol) and reacted it with carbon monoxide in the presence of Piers' borane $[HB(C_6F_5)_2]$.[12] We assume that Piers' borane carbonyl $[(C_6F_5)_2B(H)CO]$[13] was formed in situ, which then was reduced by the active $[Zr]-H$ reagent to give the zirconocene coordinated formyl hydridoborate product **2**. Compound **2** was characterized by X-ray diffraction and by solid state NMR spectroscopy. However, the compound turned out to show dynamic behavior in solution, indicating a very rapid equilibration with the $[Zr]-O-CH_2-[B]$ isomer **3**. The in situ available system **3** turned out to be highly reactive. It underwent rapid reactions with a variety of added substrates acting as a reactive oxygen/borane FLP. The zirconocene unit was just an innocent bystander that was necessary for the effective generation of the O/B pair by the carbonylation route (Scheme 1).[10]

Scheme 1. Formation of the [Zr]-formylhydridoborate 2

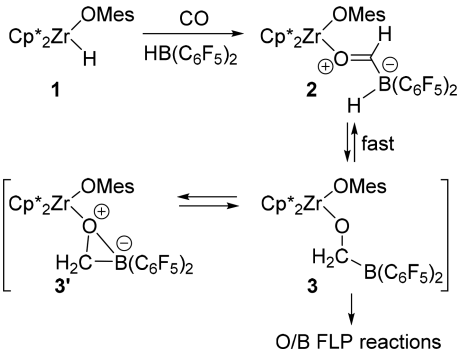

It was tempting to speculate that related reactive geminal O/B FLPs might become available by true metal-free carbonylation routes. We found that this was indeed the case by employing a special intramolecular N/B FLP for the reaction with the $CO/HB(C_6F_5)_2$ pair. The formation of the respective metal-free $-O-CH_2-[B]$ system and first reactions are described and discussed in this account.

RESULTS AND DISCUSSION

Formation and First Characterizing Reactions of the N/B FLP 7. For the purpose of this study, we used a trimethylene-bridged N/B FLP **7**[14] with a specifically designed amine Lewis base function, that, as we shall see, provides an essential chemical feature for the generation of the $-O-CH_2-[B]$ function (Scheme 2). The synthesis started from *N*-allyl-*cis*-2,6-dimethylpiperidine (**4**) that we had made by N-allylation of the respective piperidine derivative. The commercial starting

Received: January 18, 2018

DOI: 10.1021/acs.organomet.8b00035
Organometallics XXXX, XXX, XXX–XXX

Scheme 2. Synthesis of the N/B FLP 7 and H_2/D_2-Splitting Reactions

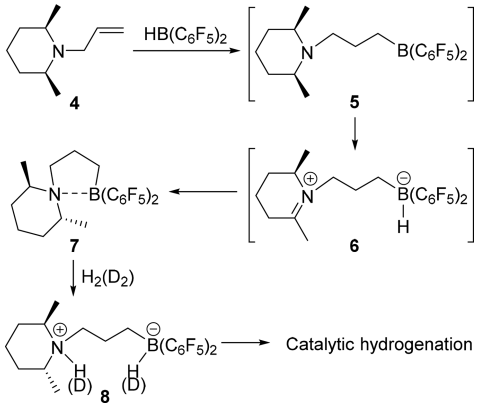

material is usually derived from hydrogenation of lutidine[15] which accounts for the *cis*-2,6-dimethyl substitution pattern. Compound **4** was then treated with Piers' borane $HB(C_6F_5)_2$, which resulted in a rapid and clean hydroboration reaction (r.t., 20 min) to give the trimethylene-bridged N/B FLP **7** (isolated in 89% yield). We note that, starting from the *cis*-dimethylpiperidine precursor **4**, we cleanly arrived at the *trans*-2,6-dimethylpiperidinyl containing N/B FLP **7**. We must, therefore, assume that a selective isomerization has taken place along the way to **7**. In view of the high hydride abstracting ability of the $-B(C_6F_5)_2$ boranes from C−H positions adjacent to nitrogen,[16] we assume that the initially formed hydroboration product **5** underwent H^- transfer to boron with iminium ion formation. Readdition is apparently fast under our typical reaction condition, and this probably provides a viable pathway to the eventual formation of the observed product **7** (Scheme 2).

Compound **7** was characterized by C,H,N-elemental analysis, by X-ray diffraction, and by NMR spectroscopy. The X-ray crystal structure analysis shows the presence of the *trans*-2,6-dimethylpiperidino group (Figure 1). It shows a chair conformation with one methyl group axially and the other equatorially oriented. Carbon atom C1 of the trimethylene bridge to boron takes an axial position at nitrogen; this leaves room for the N···B interaction in the equatorial site at nitrogen. The boron atom shows a pseudo-tetrahedral coordination

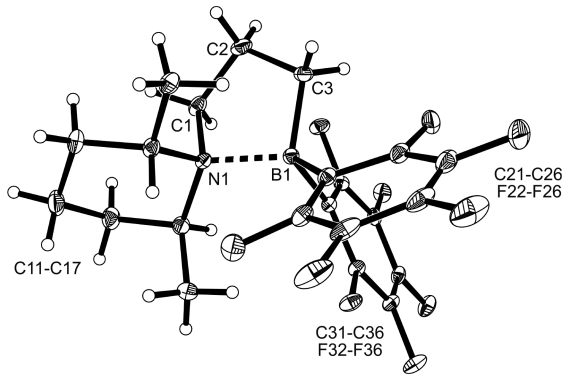

Figure 1. Molecular structure of the N/B FLP **7** (thermal ellipsoids are shown at the 15% probability level). Selected bond lengths (Å) and angles (deg): N1−C1 1.523(3), C3−B1 1.638(3); C3−B1−C31 113.2(2), C3−B1−C21 107.8(2), $\sum B1^{CCC}$ 327.4, $\sum N1^{CCC}$ 323.9, C1−N1−C11−C16 −70.6(6), C1−N1−C15−C17 176.0(2).

geometry, but we note that the N1···B1 distance is long (1.735 (3) Å) and the N/B interaction is probably weak.[5] That was confirmed by the dynamic NMR spectra of compound **7** (see below).

The ^{1}H NMR spectrum of compound **7** in CD_2Cl_2 at 213 K features the signals of a pair of inequivalent methyl substituents. It shows their adjacent C−H methine resonances at δ 4.29 and δ 2.68 ppm, respectively (with corresponding ^{13}C NMR signals at δ 64.4 and δ 53.2 ppm). Due to the chirality of the *trans*-2,6-dimethylpiperidino unit, all CH_2 hydrogens are diastereotopic. So we observed a total of 12 respective ^{1}H NMR signals and a total of 6 methylene ^{13}C NMR resonances (see the Supporting Information for details). The ^{11}B NMR resonance of compound **7** occurs at δ 3.4 ppm. The ^{19}F NMR spectrum shows four *o*-, two *p*-, and four *m*-C_6F_5 signals of the pair of diastereotopic C_6F_5 substituents at boron. Compound **7** shows dynamic NMR spectra at high temperature. The ^{19}F NMR signals of the $-B(C_6F_5)_2$ moiety eventually coalesce to a single 2:1:2 intensity set for the *o*-, *p*-, and *m*-fluorines at $T_c \sim 299$ K, which probably indicates rapid equilibration with the respective "invisible" open N/B isomer. From this behavior, we have estimated the Gibbs activation barrier of the (reversible) N···B bond dissociation at $\Delta G^{\ddagger}$ (299 K) = 12.7 ± 0.3 kcal·mol^{-1}.[17]

The FLP **7** is an active dihydrogen splitting reagent. Exposure of a solution of compound **7** in dichloromethane to a dihydrogen atmosphere (2.0 bar, r.t.) resulted in the appearance of a white precipitate within 10 min. The reaction was stirred for some time to let it go to completion. We isolated the ammonium/hydridoborate product **8** in 87% yield. It shows the typical NMR features of the backbone plus a broad ^{1}H NMR NH signal at δ 7.76 and a 1:1:1:1 intensity BH ^{1}H NMR resonance at δ 2.87, with a corresponding ^{11}B NMR feature at δ −20.5 ppm (d, $^1J_{BH} \sim 77$ Hz). We also carried out the analogous reaction with D_2 and isolated the isotopologue **8**-D_2 in 86% yield. In the ^{1}H NMR spectrum, the respective NH and BH resonances are now missing, but two broad signals appeared in the ^{2}H NMR spectrum of compound **8**-D_2 at δ 7.62 (ND) and δ 2.87 ppm (BD), respectively (for further details and the depicted NMR spectra of compound **8**/**8**-D_2, see the Supporting Information).

The X-ray crystal structure analysis of compound **8** shows the dimethylpiperidino moiety featuring one methyl group in the axial position and the other equatorially oriented. The trimethylene bridge is equatorially attached at nitrogen, which brings the newly introduced ammonium hydrogen atom in an axial position. The $[N]-(CH_2)_3-[B]$ unit features a distorted cisoid (close to doubly gauche) conformational arrangement (dihedral angles N1−C1−C2−C3 −46.4(2)°, C1−C2−C3−B1 −45.5(2)°). The boron atom B1 bears the hydride in a pseudo-tetrahedral arrangement ($\sum B1^{CCC}$ 337.7°) (Figure 2).

Compound **8** is a metal-free hydrogenation catalyst. Both the imine **9a** and the enamine **10a** were hydrogenated using 10 mol % each of the NH^+/BH^- catalyst in CD_2Cl_2 solution under mild conditions (r.t., 2.0 bar H_2, 3 d) to give the respective amine products **9b** and **10b** in practically quantitative conversion.[5a,18] Compound **8** is also a hydrogenation catalyst for the *α,β*-unsaturated ketone chalcone **11a**, albeit this hydrogenation reaction is somewhat slower.[19] With 10 mol % of the catalyst **8**, we achieved a 38% conversion under our typical conditions. It took 20 mol % of **8** to achieve a close to quantitative conversion to the saturated ketone **11b** (94%, Scheme 3; see the Supporting Information for further details).

DOI: 10.1021/acs.organomet.8b00035
Organometallics XXXX, XXX, XXX−XXX

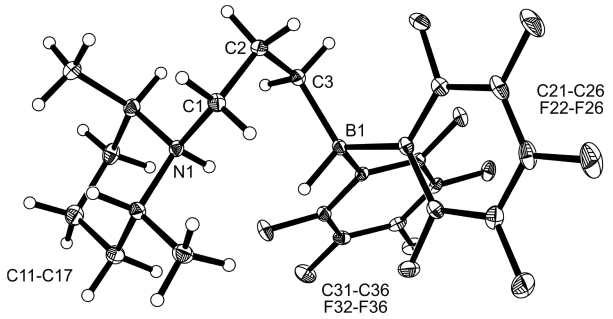

Figure 2. A view of the molecular structure of the FLP dihydrogen splitting product **8** (thermal ellipsoids are shown at the 30% probability level). Selected bond lengths (Å) and angles (deg): N1–C1 1.513(2), C1–C2 1.523(2), C2–C3 1.544(2), C3–B1 1.632(2); $\sum N1^{CCC}$ 340.0, C15–N1–C11–C16 66.1(2), C11–N1–C15–C17 −176.3(1).

Scheme 3. Catalytic Hydrogenation Using the Metal-Free NH^+/BH^- Catalyst 8

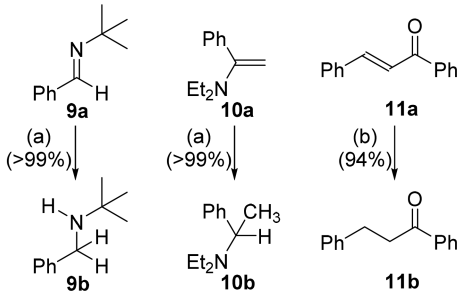

Formation of the Borataepoxide System by the FLP Carbonylation Route. The borataepoxide system **12** turned out to be an important compound of our study. It was prepared from the N/B FLP **7** by treatment with carbon monoxide and $HB(C_6F_5)_2$ under mild conditions (CH_2Cl_2, r.t., 2.0 bar CO, 1 h). Workup gave the product **12** as a white solid in 91% yield. The X-ray crystal structure analysis showed that the saturated COB containing three-membered heterocycle had been formed selectively (Figure 3). This formally anionic moiety is found coordinated to the N/B FLP boron atom (B1) through its ring oxygen atom. The oxygen coordination geometry in the solid state is trigonal pyramidal. The trimethylene bridge connects boron atom B1 with the dimethylpiperidine derived moiety, but this has lost a hydrogen atom adjacent to nitrogen to generate an endocyclic iminium ion moiety.

The ^1H NMR spectrum of compound **12** in CD_2Cl_2 solution shows the signal of the sole remaining α-hydrogen atom adjacent to nitrogen at δ 4.11 ppm. There is the iminium ion ^{13}C NMR resonance at δ 187.5 ppm. The borataepoxide CH_2 group gives rise to signals at δ 3.17 (^1H) and δ 57.5 ppm (^{13}C), respectively [cf. the $-CH_2-$B1 resonances of the trimethylene bridge occur at δ 1.12 (^1H) and δ 21.3 ppm (^{13}C)]. We found two boron resonances (δ 3.5 and δ −10.5 ppm), both being in the tetracoordinate boron range, and we monitored the ^{19}F NMR signals of a total of four $-C_6F_5$ substituents attached at the pair of boron atoms of compound **12**. We found that one pair of p-C_6F_5 signals was beginning to broaden with increasing the monitoring temperature from 263 to 299 K, which might potentially indicate a beginning equilibration of the borataepoxide ring with its ring-opened isomeric form on the NMR time scale.

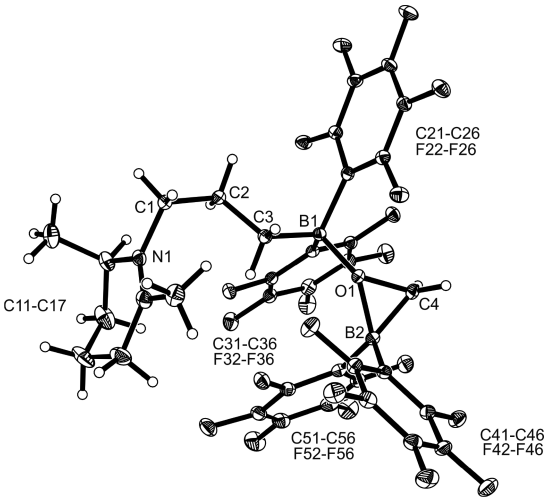

Figure 3. A view of the FLP derived borataepoxide system **12** (thermal ellipsoids are shown at the 15% probability level). Selected bond lengths (Å) and angles (deg): N1–C11 1.282(4), N1–C15 1.526(4), N1–C1 1.489(4), C1–C2 1.531(4), C2–C3 1.530(4), C3–B1 1.610(4), B1–O1 1.551(4), O1–C4 1.482(3), C4–B2 1.549(5), B2–O1 1.553(4); C11–N1–C1 123.6(3), O1–C4–B2 61.6(2), C4–B2–O1 57.1(2), B2–O1–C4 61.3(2), $\sum N1^{CCC}$ 360.1, $\sum B1^{CCC}$ 337.8, $\sum O1^{CBB}$ 326.4, N1–C1–C2–C3 −63.1(4), C1–C2–C3–B1 178.3(3).

[B]–H boranes usually do not reduce carbon monoxide, unless catalyzed or induced by hydridoboranes.[20,21] Instead, they form borane carbonyls. Typical examples are H_3B-CO[20] or $(C_6F_5)_2B(H)CO$ (**13**).[13] CO reduction by $HB(C_6F_5)_2$ had been achieved at P/B FLP templates. Some of these effects are probably used in the CO reduction by $HB(C_6F_5)_2$ at the N/B FLP system **7**, as well. We notice that the formation of the borataepoxide from CO required two hydride equivalents. One obviously originates from the added $HB(C_6F_5)_2$ reagent, and the other then must be provided by the FLP system **7**. This lets us to assume equilibration of **7** with the iminium/hydridoborate isomer **6** (Schemes 2 and 4) by the well-established hydride abstraction at the α-NCH by the adjacent active $-B(C_6F_5)_2$ borane.[16] The hydridoborate functionality might then reduce the CO group of in situ generated Piers' borane carbonyl $[(C_6F_5)_2B(H)CO]$ (**13**) to generate the borane coordinated formyl hydridoborate moiety[10,22] in the intermediate **14** (Scheme 4). Internal carbonyl reduction by the boron-hydride then leads to **15**. This can then probably undergo facile ring closure to give the observed borataepoxide ring system attached at the N/B FLP derived framework (**12**).

Compound **12** is thermally sensitive. Keeping it for 18 h in CH_2Cl_2 solution at r.t. resulted in a complete rearrangement to the product **16**, which we isolated from the workup procedure as a white solid in 95% yield. The ^{19}F NMR spectrum showed two sets of o,p,m-C_6F_5 signals in a 1:3 intensity ratio indicating the presence of a $-B(C_6F_5)$ and a $-B(C_6F_5)_3$ unit. We detect a sharp ^{11}B NMR signal in the typical borate range (δ −14.3 ppm) and a broad ^{11}B NMR feature at δ 44.7 ppm, which is typical for an oxygen bound trivalent boron center in this situation. There is a set of NMR signals of a [B]–O–CH_2–[B] unit at δ 4.43/4.32 (^1H) and δ 71.6 ppm (^{13}C). In addition, we monitored the typical NMR signals of the trimethylene-bridged N/B framework [e.g., δ 188.0 ppm (^{13}C), iminium cation].

DOI: 10.1021/acs.organomet.8b00035
Organometallics XXXX, XXX, XXX–XXX

Scheme 4. Carbon Monoxide Reduction with the N/B FLP 7

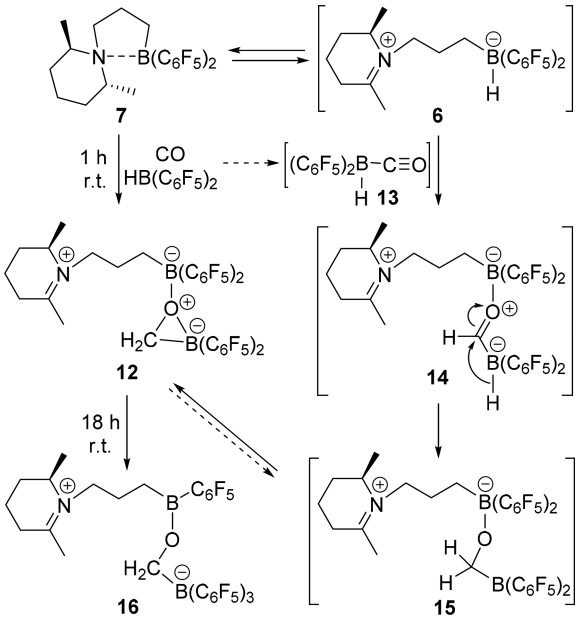

The X-ray crystal structure analysis confirmed that the product **16** was formed by C_6F_5 migration from boron atom B1 to B2 (Figure 4). Boron atom B1 consequently has one C_6F_5

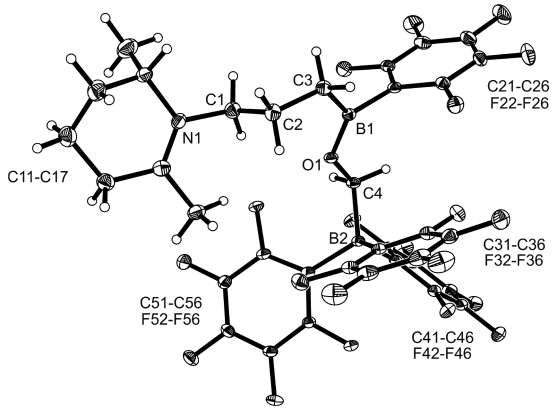

Figure 4. Molecular structure of the thermodynamic CO reduction product **16** (thermal ellipsoids are shown at the 15% probability level). Selected bond lengths (Å) and angles (deg): B1−C3 1.565(4), B1−O1 1.334(4), B1−C21 1.593(4), O1−C4 1.470(3), C4−B2 1.635(4); B2−C4−O1 111.3(2), C4−O1−B1 123.0(2), O1−B1−C3 120.3(3), $\sum B1^{OCC}$ 360.0, N1−C1−C2−C3 −165.3(4), C2−C3−B1−O1 −6.6(4), B1−O1−C4−B2 134.5(3).

group, carbon atom C3 of the trimethylene bridge to nitrogen, and the former carbonyl oxygen atom O1 bonded to it in a planar-tricoordinated geometry. The dimethylpiperidine derived nitrogen heterocycle contains an internal iminium ion function. Boron atom B2 is tetracoordinated by three C_6F_5 substituents and the CH_2 group (C4) of the [B1]−O−CH_2−[B2] bridge.

C−H Activation and H_2-Splitting. Many frustrated Lewis pairs react with the C−H acidic terminal alkynes by deprotonation to give the respective cation/alkynylborate salts,[23] and many FLPs split dihydrogen under mild reaction conditions.[1,2] Our new borataepoxide system **12** undergoes both of these reactions as well (Scheme 5).

Scheme 5. Reaction of the Borataepoxide System 12 with a Terminal Alkyne and with Dihydrogen

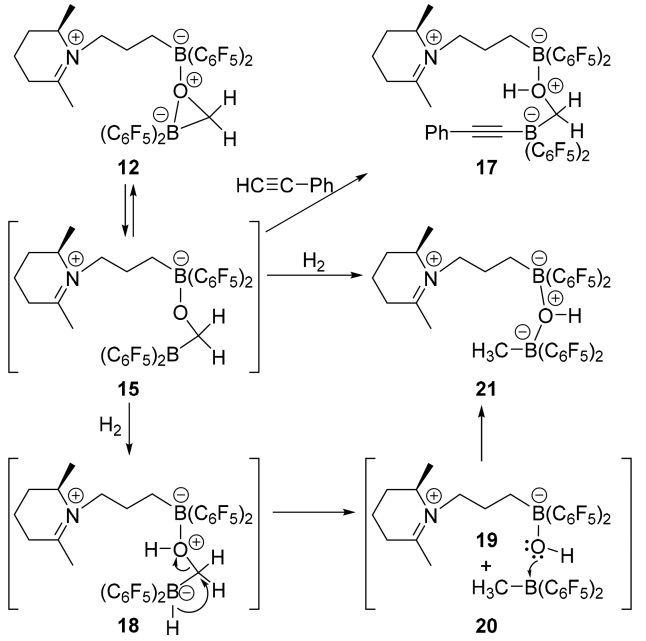

Compound **12** reacts rapidly with phenylacetylene (r.t., 1 h) in dichloromethane solution to give the C−H activation product **17** (isolated as a white solid in 92% yield). The compound is thermally sensitive, so the characterization was done at low temperature. The ^{13}C NMR spectrum of compound **17** shows the typical iminium N=C feature at δ 186.9 and a pair of [B]-acetylide carbon resonances at δ 103.7 (br, B−C≡) and δ 99.0 ppm (≡C−Ph), respectively. The compound shows a broad −OH ^1H NMR signal at 6.85 and a pair of ^{10}B NMR signals at δ 4.3 and δ −19.6 ppm. We have monitored four ^{19}F NMR *o,p,m*-sets of signals for a total of four diastereotopic C_6F_5 substituents at the pair of boron atoms (see the Supporting Information for details).

Single crystals suited for the X-ray crystal structure analysis of compound **17** were obtained at −35 °C from a dichloromethane solution layered with *n*-pentane. It confirms cleavage of the acetylene C−H bond. The proton has become bonded to the [B]−O1 oxygen atom to generate an oxonium cation moiety, and the remaining alkynyl anion has become bonded to the boron atom B2 of the former borataepoxide. The B2−acetylide moiety is close to linear as expected (Figure 5).

We performed the reaction of the borataepoxide **12** with dihydrogen at 50 bar H_2 (1 d) using a suspension in dichloromethane. Under these conditions, the competing rearrangement of **12** to **16** was sufficiently suppressed and we isolated the H_2-splitting product **21** in 83% yield. The X-ray crystal structure analysis showed again the presence of the [B1]−OH−[B2] bridged unit. In this case, the boron atom B2 has a methyl substituent bonded to it. The methyl group eventually originated from carbon monoxide, which had become first reduced to the boron bonded −O−CH_2− moiety and then further reduced by treatment with H_2 all the way to the [B2]−CH_3 structural unit (Figure 6).[24]

In solution (THF-d_8), compound **21** shows the broadened ^1H NMR OH resonance at δ 6.04 and the [B2]−CH_3 $^1H/^{13}C$ NMR signals at δ 0.42/δ 10.0 ppm. In principle, we should see the ^{19}F NMR signals of four diastereotopic C_6F_5 groups.

DOI: 10.1021/acs.organomet.8b00035
Organometallics XXXX, XXX, XXX−XXX

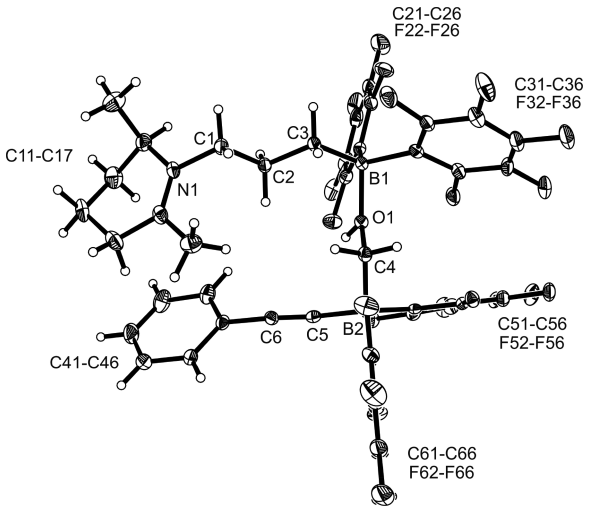

Figure 5. A view of the molecular structure of the acetylene C−H cleavage product **17** (thermal ellipsoids are shown at the 15% probability level). Selected bond lengths (Å) and angles (deg): N1−C11 1.498(6), N1−C15 1.313(6), N1−C1 1.469(5), B1−O1 1.589(6), O1−C4 1.496(5), C4−B2 1.622(6), B2−C5 1.597(6), C5−C6 1.203(5), C6−C41 1.438(6); C11−N1−C15 123.4(4), B1−O1−C4 124.2(3), O1−C4−B2 104.7(3), C4−B2−C5 104.4(3), B2−C5−C6 168.7(4), C5−C6−C41 176.7(5), $\sum N1^{CCC}$ 359.8, $\sum B1^{CCC}$ 340.7, B1−O1−C4−B2 −177.1(3), N1−C1−C2−C3 −172.3(4), C1−C2−C3−B1 176.3(4).

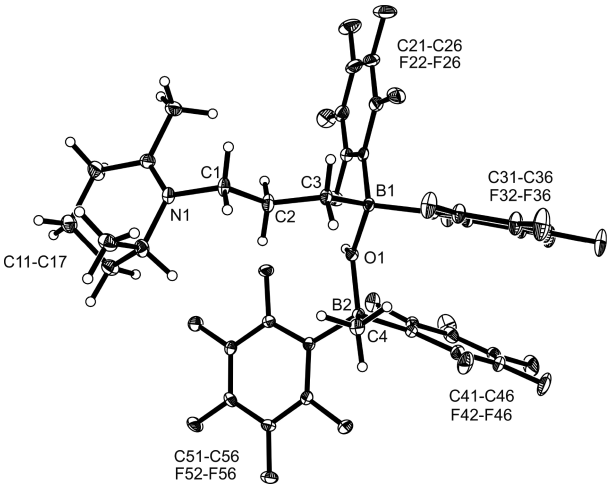

Figure 6. Molecular structure of the borataepoxide reduction product **21** (thermal ellipsoids are shown at the 30% probability level). Selected bond lengths (Å) and angles (deg): B1−O1 1.566(2), O1−B2 1.563(2), B2−C4 1.606(2); B1−O1−B2 131.5(1), O1−B2−C4 109.6(1), B1−O1−B2−C4 30.3(2).

However, we have monitored two *o,p,m*-sets of signals at 299 K (see the Supporting Information for details).

We do not know the mechanistic details of the formation of the product **21**. In principle, one might discuss two possible pathways to explain the splitting of the H−H molecule by compound **12**. One would involve a direct reaction of H_2 with the O−C bond of the strained borataepoxide. A more conventional alternative would involve the ring-opened form **15**, and a subsequent frustrated Lewis pair (FLP) pathway. The latter is depicted in Scheme 5, proceeding via the zwitterionic oxonium/hydridoborate intermediate **18**. This is set for internal nucleophilic attack by hydride on the adjacent methylene group using the good oxonium leaving group.[9] Consequently, cleavage of the O−C σ-bond would lead to a [B]−OH **19**/CH_3−$B(C_6F_5)_2$ **20** pair of products. Capture of the Lewis acidic methyl-bis(pentafluorophenyl)borane by the hydroxylborate function may then directly lead to the observed product **21**.

Carbon Dioxide Capture and Related Reactions. We had shown that the reactive formyl(hydrido)borate zirconium complex **2** added CO_2.[10,25,26] This reaction might have proceeded via the zirconoxy/borane FLP **3**/**3′**. The borataepoxide system **12** undergoes the analogous reaction in its metal-free environment. The solution of compound **12** in dichloromethane was exposed to a CO_2 atmosphere (2 bar) for 2 h at r.t. Workup involving washing with *n*-pentane gave compound **23** as a white solid, which we isolated in a yield of 96% (Scheme 6).

Scheme 6. Reaction of the Borataepoxide 12 with Carbon Dioxide

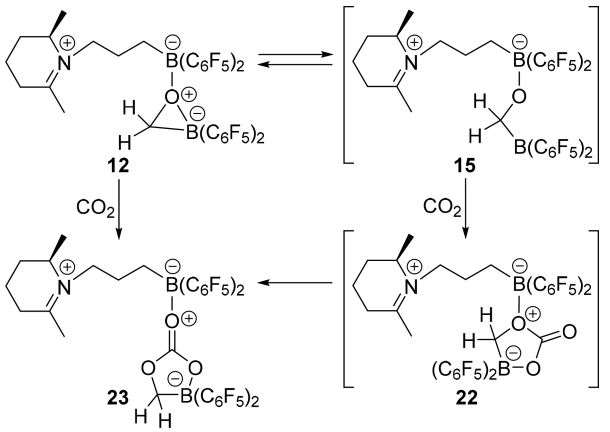

The X-ray crystal structure analysis shows that a borata-ethylenecarbonate unit was formed. The five-membered heterocyclic unit contains the B−O−CH_2 building block originating from the starting material **12** combined with a molecule of carbon dioxide. In the product **23**, the borata-carbonate carbonyl oxygen atom O1 is found bonded to the boron atom (B1) of the FLP framework (Figure 7).

Compound **23** shows the typical iminium ^{13}C NMR resonance in solution (THF-d_8) at δ 188.7 ppm. The borata-carbonate ^{13}C NMR feature was located at δ 166.4, and the endocyclic CH_2 group of this newly formed five-membered heterocycle shows $^{1}H/^{13}C$ NMR signals at δ 4.35/73.8 ppm. It seems that the boron resonances are by chance isochronous; we observed only a single broad resonance at δ 1.7 ppm in both the ^{11}B and ^{10}B NMR spectra of compound **23**. It shows two equal intensity *o,p,m*-C_6F_5 sets of ^{19}F NMR signals for the pair of $-B(C_6F_5)_2$ groups in this molecule (see the Supporting Information for details).

We assume a reaction pathway that involves endergonic equilibration of **12** with the open form **15**. This then could undergo the O/B FLP addition reaction to a C═O moiety of carbon dioxide to generate the borata-carbonate subunit in the intermediate **22**. Rearrangement to the favored carbonyl to boron Lewis acid coordinated isomer then closes the reaction cycle as depicted in Scheme 6.

The reaction of the **12** with acetonitrile (**a**) or benzonitrile (**b**) proceeds similarly.[27,28] The nitrile addition reactions yield the products **24**. We assume 1,2-addition of the −C≡N

DOI: 10.1021/acs.organomet.8b00035
Organometallics XXXX, XXX, XXX−XXX

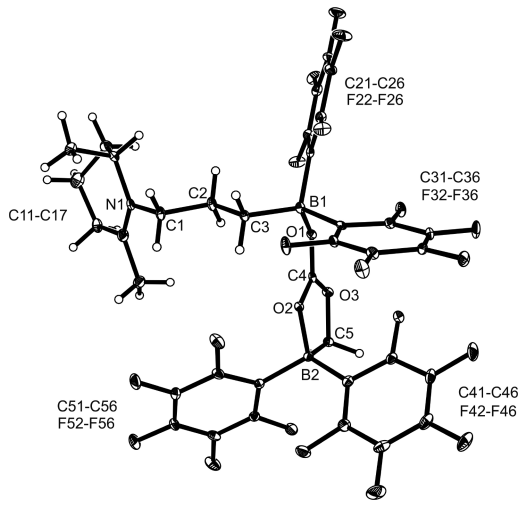

Figure 7. Molecular structure of the borata-ethylenecarbonate product **23** from the reaction of the borataepoxide **12** with carbon dioxide (thermal ellipsoids are shown at the 30% probability level). Selected bond lengths (Å) and angles (deg): B1−O1 1.573(2), O1−C4 1.255(2), C4−O2 1.285(2), C4−O3 1.310(2), B2−O2 1.548(2), B2−C5 1.644(3), C5−O3 1.480(2), N1−C11 1.300(3); B1−O1−C4 124.2(2), C4−O2−B2 110.3(2), C4−O3−C5 109.3(1), O2−B2−C5 98.5(1), B2−C5−O3 103.7(2), C5−O3−C4 109.3(1), $\sum B1^{CCC}$ 336.1, $\sum C4^{OOO}$ 360.0.

function to the O/B section of **12** to generate **26**. Both the systems in these cases then are not stable but undergo deprotonation at the methyl group of the iminium ion part of the system under our typical reaction conditions (r.t., 1 h, CH_2Cl_2) to form the observed products **24** and generate the reactive intermediate **27**. This contains an enamine functionality alongside of an active borane Lewis acid. Enamine C-addition to boron[29] then probably represents the final step in the formation of the second reaction product, the bicyclic iminium/borate zwitterion **25** (Scheme 7). The products **24** and **25** were in both cases found in a ca. 1:1 ratio.

In the acetonitrile series, we could separate the products by treatment with *n*-pentane. This left compound **25** as a white solid (isolated in 95% yield). From the *n*-pentane extract, we isolated compound **24a** (R = CH_3) in 93% yield.

We obtained single crystals of compound **25** from the acetonitrile experiment that were suited for its characterization by X-ray diffraction. The compound shows a heterobicyclo-[5.4.0]undecene-like structure. There is an iminium N=C double bond between the bridgeheads. Carbon atom C9 inside the six-membered subunit bears the methyl substituent, and the borate anion unit is part of the seven-membered substructure (Figure 8).

Scheme 7. Reaction of the O/B FLP with Nitriles

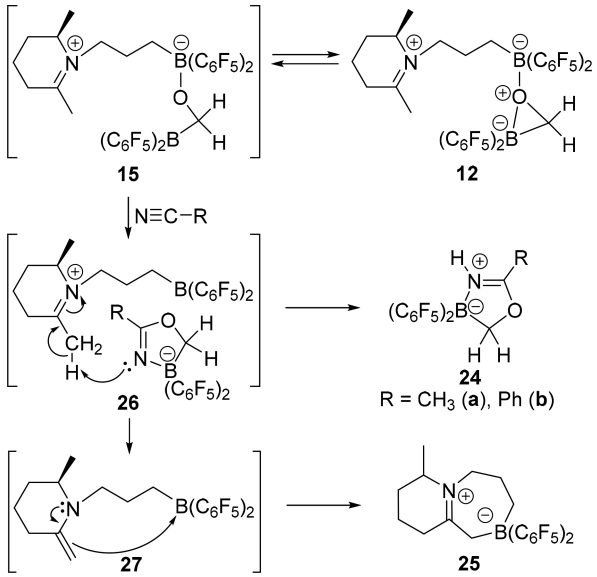

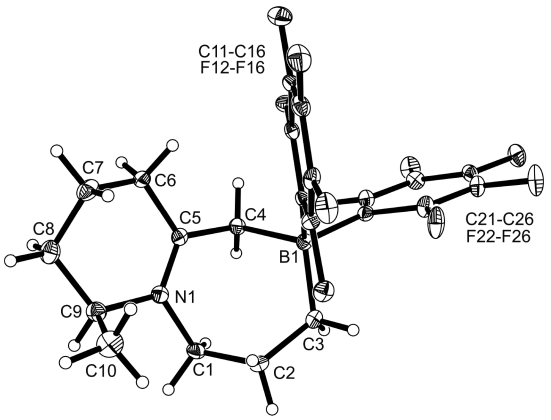

Figure 8. A projection of the molecular structure of compound **25** (thermal ellipsoids are shown at the 15% probability level). Selected bond lengths (Å) and angles (deg): N1−C5 1.295(4), N1−C1 1.483(4), B1−C3 1.628(5), B1−C4 1.688(5); C4−B1−C3 107.7(3), $\sum N1^{CCC}$ 359.9, $\sum C5^{NCC}$ 360.0, N1−C1−C2−C3 −77.7(4), C2−-C3−B1−C4 −51.8(4).

The ^{1}H NMR spectrum of compound **25** in CD_2Cl_2 at 299 K shows the methyl group signal at δ 1.33 ppm. The hydrogen atoms of the ring CH_2 groups are each pairwise diastereotopic due to the C9 carbon chirality center (atom numbering as depicted in Figure 8) as are the C_6F_5 groups at boron. These show two sets of each *o*,*p*,*m*-C_6F_5 ^{19}F NMR signals at 299 K, which both decoalesce upon lowering the monitoring temperature. The dynamic behavior indicates freezing of the rotation of the $-C_6F_5$ groups around the B−C vectors plus a lowering of the conformational mobility of the framework ring systems on the NMR time scale. The iminium ^{13}C NMR carbon resonance of compound **25** was located at δ 197.9 ppm.

Compound **24a** (R = CH_3) was characterized by C,H,N-elemental analysis and by NMR spectroscopy. The zwitterionic five-membered heterocycle shows a very simple ^{1}H NMR spectrum showing three singlets at δ 7.95 (br, 1H, NH), δ 4.75 (2H, CH_2; ^{13}C: δ 79.4), and δ 2.31 (3H, CH_3; ^{13}C: δ 16.6), respectively. The ^{11}B NMR resonance of compound **24a** was located at δ −6.8 ppm, i.e., in the typical tetracoordinate borate range, and there are three ^{19}F NMR signals of the *o*,*p*,*m*-fluorine atoms of the pair of symmetry equivalent C_6F_5 groups at boron.

The reaction of **12** with benzonitrile (1 h, r.t., CH_2Cl_2) proceeded similarly. After removal of the solvent in vacuo, treatment with *n*-pentane gave the insoluble compound **25**, which we isolated in 96% yield. The *n*-pentane extract was concentrated. Crystallization at −78 °C gave compound **24b** in 95% yield. Single crystals of **24b** were obtained from a two-layer dichloromethane/*n*-pentane mixture at −35 °C. This allowed characterization of compound **24b** by X-ray crystal structure analysis. It shows a close to planar five-membered

DOI: 10.1021/acs.organomet.8b00035
Organometallics XXXX, XXX, XXX−XXX

heterocycle with a strong internal B−N linkage and an adjacent iminium-type C═N double bond. The phenyl substituent at the ring carbon atom C2 is rotated slightly away from the central five-membered core plane of compound **24b** (Figure 9).

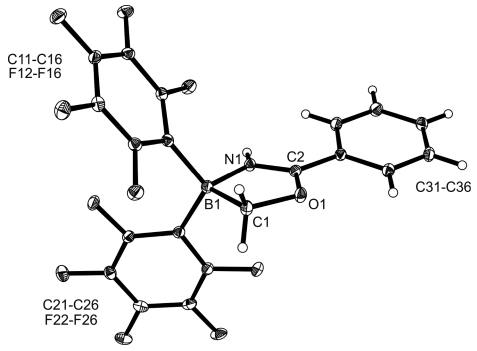

Figure 9. Molecular structure of compound **24b** (R = Ph) (thermal ellipsoids are shown at the 15% probability level). Selected bond lengths (Å) and angles (deg): B1−N1 1.564(3), N1−C2 1.292(2), C2−C31 1.462(3), C2−O1 1.310(2), O1−C1 1.494(2), C1−B1 1.645(3); N1−B1−C1 95.8(1), B1−C1−O1 105.3(1), C1−O1−C2 109.7(1), C2−N1−B1 113.7(2), $\sum B1^{CCC}$ 339.8, $\sum C2^{ONC}$ 360.0, N1−C2−C31−C32 11.2(3).

The phenyl substituted compound **24b** shows similar NMR features as **24a**. We observed the NH ^{1}H NMR resonance at δ 8.31 and the endocyclic CH_2 resonance at δ 4.96. The iminium ion ^{13}C NMR signal occurs at δ 175.0 and the ^{11}B NMR resonance is at δ −6.5 ppm.

Compound **12** reacts rapidly with benzaldehyde (1 h, r.t., CH_2Cl_2). Two equivalents of the aldehyde are consumed to let the reaction go to completion. It gives a ca. 1:1 mixture of the products **30** and **31** (Scheme 8). The compounds could be

Scheme 8. Reaction of the Borataepoxide with Benzaldehyde

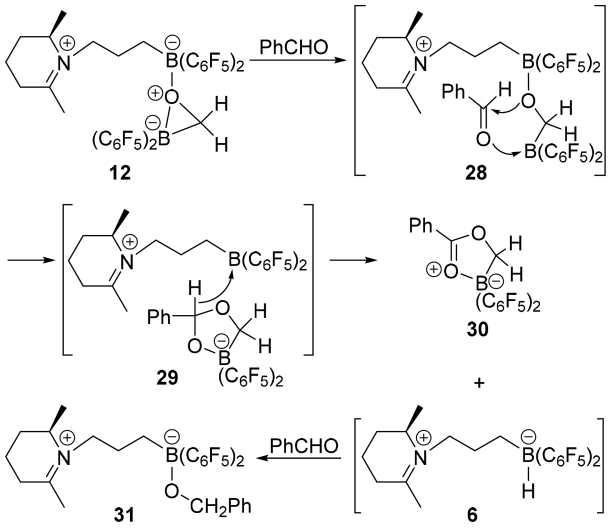

separated by treatment with *n*-pentane. Stirring the mixture with this solvent gave a suspension of the insoluble product **31**. It was collected by filtration and obtained in 93% yield. From the *n*-pentane extract, compound **30** was crystallized at −78 °C (1 h). The crystalline product was isolated in 91% yield. Both products were characterized by NMR spectroscopy and by X-ray diffraction. Compound **31** shows the typical NMR features (THF-d_8) of the trimethylene-bridged N/B backbone [δ 187.3 (C═N$^+$), δ 58.6, 26.2, 20.4 (−$(CH_2)_3$−), δ 0.1 ppm (^{11}B)]. We monitored the ^{1}H NMR signals of the newly introduced −OCH_2Ph group at boron at δ 4.29 [δ 66.2 (^{13}C)] (CH_2) and δ 7.39, 7.17, 7.04 ppm (Ph).

The X-ray crystal structure analysis has confirmed the structural assignment of the product **31**. Its structural features are unexceptional. The structure is depicted in the Supporting Information. The X-ray crystal structure analysis of product **30** shows the presence of a planar five-membered heterocycle. The phenyl substituent at carbon atom C2 is oriented almost in plane. The adjacent carbon−oxygen bonds are almost equidistant (C2−O2: 1.268(2) Å, C2−O1: 1.294(3) Å).[30] The B−C_6F_5 vectors are oriented close to eclipsed with the C1−H bonds of the adjacent CH_2 group (Figure 10).

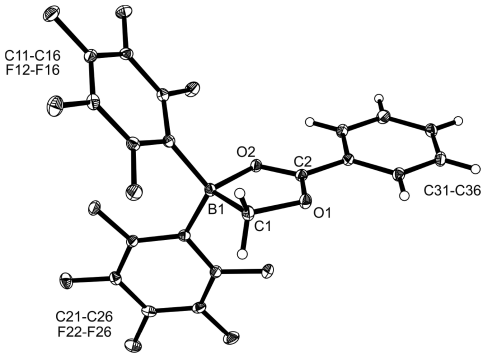

Figure 10. Molecular structure of compound **30** (thermal ellipsoids are shown at the 15% probability level). Selected bond lengths (Å) and angles (deg): B1−C1 1.636(3), B1−O2 1.566(3), O2−C2 1.268(2), C2−O1 1.294(3), O1−C1 1.493(3); B1−C1−O1 103.6(2), O1−C2−O2 118.3(2), $\sum B1^{CCC}$ 342.4, O1−C2−C11−C12 −174.3(2).

In CD_2Cl_2 solution, compound **30** shows a ^{1}H NMR singlet of the endocyclic CH_2 group at δ 4.92 (^{13}C: δ 79.0) and the resonances of the phenyl substituent at carbon C2. The carbonyl carbon shows a ^{13}C NMR signal at δ 181.1 ppm. Compound **30** features a ^{11}B NMR signal at 3.4 ppm and a single set of three ^{19}F NMR resonances of the pair of symmetry-equivalent C_6F_5 substituents at boron ($\Delta\delta^{19}F_{m,p}$ = 6.6 ppm).

We assume that compound **12** adds to the benzaldehyde carbonyl group[21c−e,31] to generate **29**. This would give the core of the eventually observed five-membered heterocycle, albeit in the wrong oxidation state. Therefore, it is likely that the active borane Lewis acid at the intermediate stage **29** (Scheme 8) serves to abstract hydride[16] from it to form the final product **30**. This reaction generates the zwitterion **6** containing an active hydridoborate function which is trapped by benzaldehyde to give the second observed product **31**.

CONCLUSIONS

[B]−H boranes usually do not reduce carbon monoxide. Instead, they may form borane carbonyls. Typical examples are the formation of the parent borane carbonyl **32** from diborane[20] and CO or the formation of Piers' borane carbonyl (**13**) from $HB(C_6F_5)_2$ and carbon monoxide. We had recently prepared this compound and characterized it by X-ray diffraction.[13] CO reduction by [B]−H boranes required a catalyst,[21] and hydridoborates had been shown to successfully execute this task (Scheme 9).

DOI: 10.1021/acs.organomet.8b00035
Organometallics XXXX, XXX, XXX−XXX

Scheme 9. Reactions of B−H Boranes with Carbon Monoxide

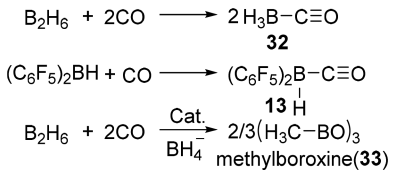

We had used the reductive power of a zirconocene hydride to achieve the [B]−CO to [B]−formyl reduction, and this had provided us with an entry to a geminal zirconoxy/B FLP system (Scheme 1).[10] Our present study was based on the necessity to provide two hydride sources for the CO reduction at the boron center under these restrictive conditions in order to achieve the reduction of carbon monoxide to the geminal $OCH_2[B]$ unit in a metal-free environment. One hydride was provided by the $HB(C_6F_5)_2$ reagent, but this could only be used in the second step of the reduction sequence. We, therefore, used the specific features of the trimethylene-bridged N/B FLP framework of compound **7** to serve as a source for a reactive borohydride reagent. This made use of the ubiquitous ability of strongly electrophilic boranes to abstract hydride from the α-position of amines to generate iminium cation/hydridoborate pairs,[16] here the respective isomer **6** from the N/B FLP **7** (Schemes 2 and 4). This sets the scene for external reduction of the in situ generated $(C_6F_5)_2B(H)CO$ by the borohydride function of **6**, followed by subsequent internal formyl hydridoborate reduction to give the borataepoxide **12**. It reacts with a variety of reagents, this including CO_2 capture to give the borata-carbonate product, splitting of dihydrogen under mild conditions, C−H cleavage of a terminal acetylene as well as nitrile and carbonyl addition reactions. The study has shown that the reactive borataepoxide can readily be generated under metal-free conditions. Its chemistry adds to the manifold of small molecule activation and binding reactions without the use of transition metal derived reagents.

EXPERIMENTAL SECTION

For general information and the spectroscopic and structural data of these new compounds, see the Supporting Information. Some of the compounds were not obtained completely pure, as judged from the results of the elemental analysis and the NMR spectra (for details, see the Supporting Information).

Synthesis of Compound 7. A solution of compound **4** (154.1 mg, 1.0 mmol) in *n*-pentane (2 mL) was added to a suspension of $HB(C_6F_5)_2$ (345.6 mg, 1.0 mmol) in *n*-pentane (20 mL), which resulted in a colorless solution within 5 min. The reaction mixture was stirred at room temperature for another 20 min, and then stored at −78 °C for 2 h to give a colorless crystalline solid, which was collected by filtration and dried in vacuo. Yield: 443.9 mg, 89%. Crystals suitable for the X-ray crystal structure analysis were obtained from a solution of compound **7** in *n*-pentane at −35 °C. Anal. Calcd for $C_{22}H_{20}BF_{10}N$ (499.2 g mol^{-1}): C, 52.93; H, 4.04; N, 2.81. Found: C, 52.42; H, 4.13; N, 2.96.

Synthesis of Compound 8. A solution of compound **7** (253.6 mg, 0.51 mmol) in CH_2Cl_2 (10 mL) was degassed by applying vacuum at r.t. Then the solution was exposed to H_2 (2.0 bar), which resulted in the appearance of a white precipitate within 10 min. The mixture was stirred at r.t. for 5 h. Then the suspension was filtered, the obtained solid was washed with *n*-pentane (3 × 3 mL) and dried in vacuo to give a white solid. Yield: 221.7 mg, 87%. Crystals suitable for the X-ray crystal structure analysis were obtained from a two-layer procedure using a solution of compound **8** in CH_2Cl_2 covered with *n*-pentane at −35 °C. Anal. Calcd for $C_{22}H_{22}BF_{10}N$ (501.2 g mol^{-1}): C, 52.72; H, 4.42; N, 2.79. Found: C, 52.62; H, 4.32; N, 2.81.

Synthesis of Compound 8-D_2. A solution of compound **7** (180.3 mg, 0.36 mmol) in CH_2Cl_2 (5 mL) was degassed by applying vacuum at r.t. Then the solution was exposed to D_2 (1.0 bar), which resulted in the formation of a white precipitate within 10 min. The mixture was stirred at r.t. for 5 h. Then the suspension was filtered, the obtained solid material was washed with *n*-pentane (3 × 3 mL) and dried in vacuo to give a white solid. Yield: 156.3 mg, 86%.

Catalytic Hydrogenation. *Procedure A*: In a glovebox with an argon atmosphere, compound **8** (0.1 equiv) and a substrate (1.0 equiv) were dissolved in CD_2Cl_2 (1.5 mL), which was then transferred to an autoclave. The solution was stirred at r.t. for 3 days under a H_2 atmosphere (50 bar). Product conversion was estimated by ^{1}H NMR spectroscopy by integration. *Procedure B*: In a glovebox with an argon atmosphere, compound **8** (0.1 equiv) and a substrate (1.0 equiv) were dissolved in CD_2Cl_2 (1.5 mL), which was then transferred to a Schlenk flask. The solution was degassed by applying vacuum carefully at −78 °C, then stirred at r.t. for 3 days under a H_2 atmosphere (2.0 bar). Product conversion was estimated by ^{1}H NMR spectroscopy by integration.

Synthesis of Compound 12. Compound **7** (237.5 mg, 0.48 mmol) and $HB(C_6F_5)_2$ (165.1 mg, 0.48 mmol) were weighed together and dissolved in CH_2Cl_2 (15 mL) (10 mL). The mixture was degassed by applying vacuum carefully at r.t. Then the solution was exposed to CO (2.0 bar). The mixture was stirred at r.t. for 1 h. After that, all the volatiles were removed in vacuo, and the residue was washed with *n*-pentane (3 × 5 mL) and dried in vacuo to give a white solid. Yield: 378.2 mg, 91%. Crystals suitable for the X-ray crystal structure analysis were obtained from a two-layer procedure using a solution of compound **12** in the mixture of CH_2Cl_2 and toluene (v/v = 1:1) covered with *n*-pentane at −35 °C. Anal. Calcd for $C_{35}H_{21}B_2F_{20}NO$ (873.1 g mol^{-1}): C, 48.15; H, 2.42; N, 1.60. Found: C, 48.07; H, 2.41; N, 1.56.

Synthesis of Compound 16. A solution of compound **12** (503.6 mg, 0.50 mmol) in CH_2Cl_2 (25 mL) was stirred at room temperature for 18 h. Then the solvent was removed in vacuo and the obtained residue was washed with *n*-pentane (3 × 5 mL) and dried in vacuo to give a white solid. Yield: 478.5 mg, 95%. Crystals suitable for the X-ray crystal structure analysis were obtained from a two-layer procedure using a solution of compound **16** in CH_2Cl_2 covered with *n*-pentane at −35 °C. Anal. Calcd for $C_{35}H_{21}B_2F_{20}NO$ (873.1 g mol^{-1}): C, 48.15; H, 2.42; N, 1.60. Found: C, 47.92; H, 2.51; N, 1.78.

Synthesis of Compound 17. Phenylacetylene (30.6 mg, 0.30 mmol) in CH_2Cl_2 (1 mL) was added to a suspension of compound **12** (236.3 mg, 0.27 mmol) in CH_2Cl_2 (10 mL). The mixture was stirred at room temperature for 1 h. Then all the volatiles were removed in vacuo. The obtained residue was washed with *n*-pentane (3 × 3 mL) and dried in vacuo to give a white solid. Yield: 242.9 mg, 92%. Crystals suitable for the X-ray crystal structure analysis were obtained from a two-layer procedure using a solution of compound **17** in CH_2Cl_2 covered with *n*-pentane at −35 °C. Anal. Calcd for $C_{43}H_{27}B_2F_{20}NO$ (975.3 g mol^{-1}): C, 52.96; H, 2.79; N, 1.44. Found: C, 51.79; H, 2.71; N, 1.27.

Synthesis of Compound 21. Compound **12** (296.3 mg, 0.30 mmol) was suspended in CH_2Cl_2 (10 mL) and stirred at r.t. under a H_2 atmosphere (50 bar) in an autoclave for 1 day. Then the solution was transferred into a Schlenk flask and *n*-pentane (30 mL) was added to give a white precipitate. The suspension was filtered and the obtained solid material was washed with *n*-pentane (3 × 3 mL) and dried in vacuo to give a white solid. Yield: 246.5 mg, 83%. Crystals suitable for the X-ray crystal structure analysis were obtained from a two-layer procedure using a solution of compound **21** in CH_2Cl_2 covered with *n*-pentane at −35 °C. Anal. Calcd for $C_{35}H_{23}B_2F_{20}NO$ (875.2 g mol^{-1}): C, 48.03; H, 2.65; N, 1.60. Found: C, 48.05; H, 2.33; N, 1.48.

Synthesis of Compound 23. A solution of compound **12** (265.1 mg, 0.30 mmol) in CH_2Cl_2 (20 mL) was degassed by applying vacuum carefully at r.t. Then the solution was exposed to CO_2 (2.0 bar) and the mixture was stirred at r.t. for 2 h. After removal of all the volatiles

DOI: 10.1021/acs.organomet.8b00035
Organometallics XXXX, XXX, XXX−XXX

in vacuo, the obtained residue was washed with *n*-pentane (3 × 3 mL) and dried in vacuo to give a white solid. Yield: 267.3 mg, 96%. Crystals suitable for the X-ray crystal structure analysis were obtained from a two-layer procedure using a solution of compound **23** in THF covered with *n*-pentane at −35 °C. Anal. Calcd for $C_{36}H_{21}B_2F_{20}NO_3$ (917.1 g mol^{-1}): C, 47.14; H, 2.31; N, 1.53. Found: C, 46.73; H, 2.26; N, 1.53.

Synthesis of Compounds 24a and 25. Acetonitrile (29.6 mg, 0.72 mmol) in CH_2Cl_2 (1 mL) was added to a suspension of compound **12** (573.2 mg, 0.66 mmol) in CH_2Cl_2 (10 mL). The mixture was stirred at room temperature for 1 h. Then all the volatiles were removed in vacuo. The obtained residue was extracted with *n*-pentane (3 × 30 mL). The white solid was collected by filtration and dried in vacuo. It was identified as compound **25** (Yield: 310.2 mg, 95%). Crystals suitable for the X-ray crystal structure analysis were obtained from a two-layer procedure using a solution of compound **25** in CH_2Cl_2 covered with *n*-pentane at −35 °C. Anal. Calcd for $C_{22}H_{18}BF_{10}N$ (compound **25**, 497.2 g mol^{-1}): C, 53.15; H, 3.65; N, 2.82. Found: C, 52.50; H, 3.37; N, 3.00. The *n*-pentane solution was collected, concentrated to ca. 10 mL, and then stored at −78 °C for 1 h to give a colorless crystalline solid, which was collected by filtration and dried in vacuo to give a white solid (compound **24a** Yield: 254.6 mg, 93%). Anal. Calcd for $C_{15}H_6BF_{10}NO$ (compound **24a**, 417.0 g mol^{-1}): C, 43.20; H, 1.45; N, 3.36. Found: C, 43.00; H, 1.36; N, 3.38.

Synthesis of Compounds 24b and 25. Benzonitrile (61.9 mg, 0.60 mmol) in CH_2Cl_2 (1 mL) was added to a suspension of compound **12** (463.5 mg, 0.53 mmol) in CH_2Cl_2 (10 mL). The mixture was stirred at room temperature for 1 h. Then all the volatiles were removed in vacuo. The obtained residue was extracted with *n*-pentane (3 × 30 mL). The white solid was obtained by filtration and dried in vacuo, which was identified as compound **25** (Yield: 253.3 mg, 96%, characterization see above). The *n*-pentane solution was collected, concentrated to ca. 10 mL, and then stored at −78 °C for 1 h to give a colorless crystalline solid, which was collected by filtration and dried in vacuo to give a white solid (compound **24b**, Yield: 241.6 mg, 95%). Crystals suitable for the X-ray crystal structure analysis were obtained from a two-layer procedure using a solution of compound **24b** in CH_2Cl_2 covered with *n*-pentane at −35 °C. Anal. Calcd for $C_{20}H_8BF_{10}NO$ (compound **24b**, 479.1 g mol^{-1}): C, 50.14; H, 1.68; N, 2.92. Found: C, 50.08; H, 1.81; N, 2.73.

Synthesis of Compounds 30 and 31. Benzaldehyde (106.5 mg, 1.00 mmol) in CH_2Cl_2 (1 mL) was added to a suspension of compound **12** (436.6 mg, 0.50 mmol) in CH_2Cl_2 (10 mL). The mixture was stirred at room temperature for 1 h. Then all the volatiles were removed in vacuo. The obtained residue was extracted with *n*-pentane (3 × 30 mL). The white solid was obtained by filtration and dried in vacuo, which was identified as compound **31** (Yield: 281.5 mg, 93%). Crystals suitable for the X-ray crystal structure analysis were obtained from a two-layer procedure using a solution of compound **31** in CH_2Cl_2 covered with *n*-pentane at −35 °C. Anal. Calcd for $C_{29}H_{26}BF_{10}NO$ (compound **31**, 605.3 g mol^{-1}): C, 57.54; H, 4.33; N, 2.31. Found: C, 56.77; H, 4.54; N, 2.47. The *n*-pentane solution was collected, concentrated to ca. 10 mL, and then stored at −78 °C for 1 h to give a colorless crystalline solid, which was collected by filtration and dried in vacuo to give a white solid (compound **30**, Yield: 218.3 mg, 91%). Crystals suitable for the X-ray crystal structure analysis were obtained from a two-layer procedure using a solution of compound **30** in CH_2Cl_2 covered with *n*-pentane at −35 °C. Anal. Calcd for $C_{20}H_7BF_{10}O_2$ (compound **30**, 480.1 g mol^{-1}): C, 50.04; H, 1.47. Found: C, 49.70; H, 1.28.

■ ASSOCIATED CONTENT

Supporting Information

The Supporting Information is available free of charge on the ACS Publications website at DOI: 10.1021/acs.organomet.8b00035.

Experimental details and characterization data (PDF)

Accession Codes

CCDC 1589587−1589597 contain the supplementary crystallographic data for this paper. These data can be obtained free of charge via www.ccdc.cam.ac.uk/data_request/cif, or by emailing data_request@ccdc.cam.ac.uk, or by contacting The Cambridge Crystallographic Data Centre, 12 Union Road, Cambridge CB2 1EZ, UK; fax: +44 1223 336033.

■ AUTHOR INFORMATION

Corresponding Author

*E-mail: erker@uni-muenster.de.

ORCID

Gerald Kehr: 0000-0002-5196-2491

Gerhard Erker: 0000-0003-2488-3699

Notes

The authors declare no competing financial interest.

■ ACKNOWLEDGMENTS

Financial support from the Deutsche Forschungsgemeinschaft is gratefully acknowledged.

■ REFERENCES

(1) (a) Welch, G. C.; Juan, R. R. S.; Masuda, J. D.; Stephan, D. W. *Science* **2006**, *314*, 1124. (b) Welch, G. C.; Stephan, D. W. *J. Am. Chem. Soc.* **2007**, *129*, 1880. (c) Spies, P.; Erker, G.; Kehr, G.; Bergander, K.; Fröhlich, R.; Grimme, S.; Stephan, D. W. *Chem. Commun.* **2007**, 5072.

(2) (a) *Frustrated Lewis Pairs I*; Erker, G., Stephan, D. W., Eds.; Springer Press: Heidelberg, 2013; Vol. *332*. (b) *Frustrated Lewis Pairs II*; Erker, G., Stephan, D. W., Eds.; Springer Press: Heidelberg, 2013; Vol. *334*. (c) Stephan, D. W. *J. Am. Chem. Soc.* **2015**, *137*, 10018. (d) Stephan, D. W. *Acc. Chem. Res.* **2015**, *48*, 306. (e) Stephan, D. W.; Erker, G. *Angew. Chem., Int. Ed.* **2015**, *54*, 6400. (f) Stephan, D. W. *Science* **2016**, *354*, aaf7229.

(3) (a) Dureen, M. A.; Stephan, D. W. *J. Am. Chem. Soc.* **2010**, *132*, 13559. (b) Sajid, M.; Lawzer, A.; Dong, W.; Rosorius, C.; Sander, W.; Schirmer, B.; Grimme, S.; Daniliuc, C. G.; Kehr, G.; Erker, G. *J. Am. Chem. Soc.* **2013**, *135*, 18567. (c) Ekkert, O.; Miera, G. G.; Wiegand, T.; Eckert, H.; Schirmer, B.; Petersen, J. L.; Daniliuc, C. G.; Fröhlich, R.; Grimme, S.; Kehr, G.; Erker, G. *Chem. Sci.* **2013**, *4*, 2657.

(4) (a) McCahill, J. S. J.; Welch, G. C.; Stephan, D. W. *Angew. Chem., Int. Ed.* **2007**, *46*, 4968. (b) Geier, S. J.; Gilbert, T. M.; Stephan, D. W. *J. Am. Chem. Soc.* **2008**, *130*, 12632. (c) Zhao, X.; Stephan, D. W. *J. Am. Chem. Soc.* **2011**, *133*, 12448. (d) Bertini, F.; Lyaskovskyy, V.; Timmer, B. J. J.; de Kanter, F. J. J.; Lutz, M.; Ehlers, A. W.; Slootweg, J. C.; Lammertsma, K. *J. Am. Chem. Soc.* **2012**, *134*, 201. (e) Courtemanche, M.-A.; Légaré, M.-A.; Maron, L.; Fontaine, F.-G. *J. Am. Chem. Soc.* **2013**, *135*, 9326. (f) Courtemanche, M.-A.; Légaré, M.-A.; Maron, L.; Fontaine, F.-G. *J. Am. Chem. Soc.* **2014**, *136*, 10708. (g) Liu, L.; Cao, L. L.; Shao, Y.; Ménard, G.; Stephan, D. W. *Chem.* **2017**, *3*, 259.

(5) (a) Schwendemann, S.; Fröhlich, R.; Kehr, G.; Erker, G. *Chem. Sci.* **2011**, *2*, 1842. (b) Voss, T.; Mahdi, T.; Otten, E.; Fröhlich, R.; Kehr, G.; Stephan, D. W.; Erker, G. *Organometallics* **2012**, *31*, 2367. (c) Xu, B.-H.; Bussmann, K.; Fröhlich, R.; Daniliuc, C. G.; Brandenburg, J. G.; Grimme, S.; Kehr, G.; Erker, G. *Organometallics* **2013**, *32*, 6745.

(6) (a) Roesler, R.; Piers, W. E.; Parvez, M. *J. Organomet. Chem.* **2003**, *680*, 218. (b) Sumerin, V.; Schulz, F.; Atsumi, M.; Wang, C.; Nieger, M.; Leskelä, M.; Repo, T.; Pyykkö, P.; Rieger, B. *J. Am. Chem. Soc.* **2008**, *130*, 14117. (c) Sumerin, V.; Schulz, F.; Nieger, M.; Leskelä, M.; Repo, T.; Rieger, B. *Angew. Chem., Int. Ed.* **2008**, *47*, 6001. (d) Chernichenko, K.; Nieger, M.; Leskelä, M.; Repo, T. *Dalton Trans.* **2012**, *41*, 9029. (e) Winkelhaus, D.; Neumann, B.; Stammler, H.-G.; Berger, R. J. F.; Vishnevskiy, Y. V.; Mitzel, N. W. *Chem.—Eur. J.* **2012**, *18*, 9312. (f) Courtemanche, M.-A.; Pulis, A. P.; Rochette, É.; Légaré,

DOI: 10.1021/acs.organomet.8b00035
Organometallics XXXX, XXX, XXX−XXX

M.-A.; Stephan, D. W.; Fontaine, F.-G. *Chem. Commun.* **2015**, *51*, 9797. (g) Lindqvist, M.; Borre, K.; Axenov, K.; Kótai, B.; Nieger, M.; Leskelä, M.; Pápai, I.; Repo, T. *J. Am. Chem. Soc.* **2015**, *137*, 4038. (h) Chernichenko, K.; Kótai, B.; Pápai, I.; Zhivonitko, V.; Nieger, M.; Leskelä, M.; Repo, T. *Angew. Chem., Int. Ed.* **2015**, *54*, 1749. (i) Körte, L. A.; Blomeyer, S.; Heidemeyer, S.; Mix, A.; Neumann, B.; Mitzel, N. W. *Chem. Commun.* **2016**, *52*, 9949. (j) Lavergne, J. L.; Jayaraman, A.; Castro, L. C. M.; Rochette, É.; Fontaine, F.-G. *J. Am. Chem. Soc.* **2017**, *139*, 14714.

(7) (a) Holschumacher, D.; Bannenberg, T.; Hrib, C. G.; Jones, P. G.; Tamm, M. *Angew. Chem., Int. Ed.* **2008**, *47*, 7428. (b) Chase, P. A.; Stephan, D. W. *Angew. Chem., Int. Ed.* **2008**, *47*, 7433. (c) Alcarazo, M.; Gomez, C.; Holle, S.; Goddard, R. *Angew. Chem., Int. Ed.* **2010**, *49*, 5788. (d) Inés, B.; Holle, S.; Goddard, R.; Alcarazo, M. *Angew. Chem., Int. Ed.* **2010**, *49*, 8389. (e) Kolychev, E. L.; Bannenberg, T.; Freytag, M.; Daniliuc, C. G.; Jones, P. G.; Tamm, M. *Chem.—Eur. J.* **2012**, *18*, 16938.

(8) (a) Appelt, C.; Westenberg, H.; Bertini, F.; Ehlers, A. W.; Slootweg, J. C.; Lammertsma, K.; Uhl, W. *Angew. Chem., Int. Ed.* **2011**, *50*, 3925. (b) Flynn, S. R.; Wass, D. F. *ACS Catal.* **2013**, *3*, 2574. (c) Holthausen, M. H.; Bayne, J. M.; Mallov, I.; Dobrovetsky, R.; Stephan, D. W. *J. Am. Chem. Soc.* **2015**, *137*, 7298. (d) Devillard, M.; Declercq, R.; Nicolas, E.; Ehlers, A. W.; Backs, J.; Saffon-Merceron, N.; Bouhadir, G.; Slootweg, J. C.; Uhl, W.; Bourissou, D. *J. Am. Chem. Soc.* **2016**, *138*, 4917. (e) Campos, J. *J. Am. Chem. Soc.* **2017**, *139*, 2944.

(9) (a) Hounjet, L. J.; Bannwarth, C.; Garon, C. N.; Caputo, C. B.; Grimme, S.; Stephan, D. W. *Angew. Chem., Int. Ed.* **2013**, *52*, 7492. (b) Scott, D. J.; Fuchter, M. J.; Ashley, A. E. *Angew. Chem., Int. Ed.* **2014**, *53*, 10218. (c) Mahdi, T.; Stephan, D. W. *J. Am. Chem. Soc.* **2014**, *136*, 15809. (d) Scott, D. J.; Fuchter, M. J.; Ashley, A. E. *J. Am. Chem. Soc.* **2014**, *136*, 15813. (e) Hansmann, M. M.; Melen, R. L.; Rominger, F.; Hashmi, A. S. K.; Stephan, D. W. *J. Am. Chem. Soc.* **2014**, *136*, 777. (f) Gyömöre, Á.; Bakos, M.; Földes, T.; Pápai, I.; Domján, A.; Soós, T. *ACS Catal.* **2015**, *5*, 5366. (g) Scott, D. J.; Simmons, T. R.; Lawrence, E. J.; Wildgoose, G. G.; Fuchter, M. J.; Ashley, A. E. *ACS Catal.* **2015**, *5*, 5540.

(10) Jian, Z.; Kehr, G.; Daniliuc, C. G.; Wibbeling, B.; Wiegand, T.; Siedow, M.; Eckert, H.; Bursch, M.; Grimme, S.; Erker, G. *J. Am. Chem. Soc.* **2017**, *139*, 6474.

(11) (a) Wolczanski, P. T.; Bercaw, J. E. *Acc. Chem. Res.* **1980**, *13*, 121. (b) Miller, F. D.; Sanner, R. D. *Organometallics* **1988**, *7*, 818.

(12) (a) Parks, D. J.; von H. Spence, R. E.; Piers, W. E. *Angew. Chem., Int. Ed. Engl.* **1995**, *34*, 809. (b) Parks, D. J.; Piers, W. E.; Yap, G. P. A. *Organometallics* **1998**, *17*, 5492.

(13) Sajid, M.; Kehr, G.; Daniliuc, C. G.; Erker, G. *Angew. Chem., Int. Ed.* **2014**, *53*, 1118.

(14) See for a comparison: Wang, T.; Kehr, G.; Liu, L.; Grimme, S.; Daniliuc, C. G.; Erker, G. *J. Am. Chem. Soc.* **2016**, *138*, 4302.

(15) Lunn, G.; Sansone, E. B. *J. Org. Chem.* **1986**, *51*, 513.

(16) (a) Focante, F.; Mercandelli, P.; Sironi, A.; Resconi, L. *Coord. Chem. Rev.* **2006**, *250*, 170. (b) Sumerin, V.; Chernichenko, K.; Nieger, M.; Leskelä, M.; Rieger, B.; Repo, T. *Adv. Synth. Catal.* **2011**, *353*, 2093. (c) Wang, T.; Liu, L.; Grimme, S.; Daniliuc, C. G.; Kehr, G.; Erker, G. *Chem.—Asian J.* **2016**, *11*, 1394.

(17) See for a comparison: Wang, X.; Kehr, G.; Daniliuc, C. G.; Erker, G. *J. Am. Chem. Soc.* **2014**, *136*, 3293.

(18) See for a comparison: (a) Chase, P. A.; Welch, G. C.; Jurca, T.; Stephan, D. W. *Angew. Chem., Int. Ed.* **2007**, *46*, 8050. (b) Spies, P.; Schwendemann, S.; Lange, S.; Kehr, G.; Fröhlich, R.; Erker, G. *Angew. Chem., Int. Ed.* **2008**, *47*, 7543.

(19) (a) Erős, G.; Mehdi, H.; Pápai, I.; Rokob, T. A.; Király, P.; Tárkányi, G.; Soós, T. *Angew. Chem., Int. Ed.* **2010**, *49*, 6559. (b) Xu, B.-H.; Kehr, G.; Fröhlich, R.; Wibbeling, B.; Schirmer, B.; Grimme, S.; Erker, G. *Angew. Chem., Int. Ed.* **2011**, *50*, 7183. (c) Inés, B.; Palomas, D.; Holle, S.; Steinberg, S.; Nicasio, J. A.; Alcarazo, M. *Angew. Chem., Int. Ed.* **2012**, *51*, 12367. (d) Greb, L.; Daniliuc, C.-G.; Bergander, K.; Paradies, J. *Angew. Chem., Int. Ed.* **2013**, *52*, 5876.

(20) Burg, A. B.; Schlesinger, H. I. *J. Am. Chem. Soc.* **1937**, *59*, 780.

(21) (a) Rathke, M. W.; Brown, H. C. *J. Am. Chem. Soc.* **1966**, *88*, 2606. See for a comparison: (b) Yalpani, M.; Köster, R. *J. Organomet. Chem.* **1992**, *434*, 133. (c) Hillman, M. E. D. *J. Am. Chem. Soc.* **1962**, *84*, 4715. (d) Hillman, M. E. D. *J. Am. Chem. Soc.* **1963**, *85*, 982. (e) Brown, H. C.; Hubbard, J. L. *J. Org. Chem.* **1979**, *44*, 467. (f) Brown, H. C. *Acc. Chem. Res.* **1969**, *2*, 65.

(22) (a) Berkefeld, A.; Piers, W. E.; Parvez, M.; Castro, L.; Maron, L.; Eisenstein, O. *J. Am. Chem. Soc.* **2012**, *134*, 10843. (b) Dobrovetsky, R.; Stephan, D. W. *J. Am. Chem. Soc.* **2013**, *135*, 4974. (c) Sajid, M.; Elmer, L.-M.; Rosorius, C.; Daniliuc, C. G.; Grimme, S.; Kehr, G.; Erker, G. *Angew. Chem., Int. Ed.* **2013**, *52*, 2243.

(23) (a) Dureen, M. A.; Stephan, D. W. *J. Am. Chem. Soc.* **2009**, *131*, 8396. (b) Mömming, C. M.; Frömel, S.; Kehr, G.; Fröhlich, R.; Grimme, S.; Erker, G. *J. Am. Chem. Soc.* **2009**, *131*, 12280. (c) Dureen, M. A.; Brown, C. C.; Stephan, D. W. *Organometallics* **2010**, *29*, 6594.

(24) For FLP CO reduction beyond the B-formyl stage, see, e.g.: (a) Miller, A. J. M.; Labinger, J. A.; Bercaw, J. E. *J. Am. Chem. Soc.* **2010**, *132*, 3301. (b) Chapman, A. M.; Haddow, M. F.; Wass, D. F. *J. Am. Chem. Soc.* **2011**, *133*, 18463. (c) Ashley, A. E.; O'Hare, D. *Top. Curr. Chem.* **2012**, *334*, 191. (d) Wang, L.; Zhang, S.; Hasegawa, Y.; Daniliuc, C. G.; Kehr, G.; Erker, G. *Chem. Commun.* **2017**, *53*, 5499.

(25) For other FLP CO_2 addition reactions, see, e.g.: (a) Mömming, C. M.; Otten, E.; Kehr, G.; Fröhlich, R.; Grimme, S.; Stephan, D. W.; Erker, G. *Angew. Chem., Int. Ed.* **2009**, *48*, 6643. (b) Peuser, I.; Neu, R. C.; Zhao, X.; Ulrich, M.; Schirmer, B.; Tannert, J. A.; Kehr, G.; Fröhlich, R.; Grimme, S.; Erker, G.; Stephan, D. W. *Chem.—Eur. J.* **2011**, *17*, 9640. (c) Stephan, D. W.; Erker, G. *Chem. Sci.* **2014**, *5*, 2625.

(26) For FLP CO_2 reduction reactions, see also: (a) Ashley, A. E.; Thompson, A. L.; O'Hare, D. *Angew. Chem., Int. Ed.* **2009**, *48*, 9839. (b) Berkefeld, A.; Piers, W. E.; Parvez, M. *J. Am. Chem. Soc.* **2010**, *132*, 10660. (c) Chen, J.; Falivene, L.; Caporaso, L.; Cavallo, L.; Chen, E. Y.-X. *J. Am. Chem. Soc.* **2016**, *138*, 5321. (d) Bontemps, S. *Coord. Chem. Rev.* **2016**, *308*, 117.

(27) (a) Keweloh, L.; Klöcker, H.; Würthwein, E.-U.; Uhl, W. *Angew. Chem., Int. Ed.* **2016**, *55*, 3212. (b) Jian, Z.; Kehr, G.; Daniliuc, C. G.; Wibbeling, B.; Erker, G. *Dalton Trans.* **2017**, *46*, 11715. (c) Möricke, J.; Wibbeling, B.; Daniliuc, C. G.; Kehr, G.; Erker, G. *Philos. Trans. R. Soc., A* **2017**, *375*, 20170015.

(28) (a) Stute, A.; Kehr, G.; Daniliuc, C. G.; Fröhlich, R.; Erker, G. *Dalton Trans.* **2013**, *42*, 4487. (b) Elmer, L.-M.; Kehr, G.; Daniliuc, C. G.; Siedow, M.; Eckert, H.; Tesch, M.; Studer, A.; Williams, K.; Warren, T. H.; Erker, G. *Chem.—Eur. J.* **2017**, *23*, 6056.

(29) (a) Schwendemann, S.; Oishi, S.; Saito, S.; Fröhlich, R.; Kehr, G.; Erker, G. *Chem.—Asian J.* **2013**, *8*, 212. (b) Wang, T.; Wang, L.; Daniliuc, C. G.; Samigullin, K.; Wagner, M.; Kehr, G.; Erker, G. *Chem. Sci.* **2017**, *8*, 2457.

(30) Liu, Y.-L.; Kehr, G.; Daniliuc, C. G.; Erker, G. *Chem. Sci.* **2017**, *8*, 1097.

(31) (a) Mömming, C. M.; Kehr, G.; Wibbeling, B.; Fröhlich, R.; Erker, G. *Dalton Trans.* **2010**, *39*, 7556. (b) Rosorius, C.; Möricke, J.; Wibbeling, B.; McQuilken, A. C.; Warren, T. H.; Daniliuc, C. G.; Kehr, G.; Erker, G. *Chem.—Eur. J.* **2016**, *22*, 1103.

DOI: 10.1021/acs.organomet.8b00035
Organometallics XXXX, XXX, XXX−XXX